Tensile Properties of $CaCO_3$-Filled Polyethylenes

V. P. CHACKO,* R. J. FARRIS, and F. E. KARASZ, *Polymer Science and Engineering, University of Massachusetts, Amherst, Massachusetts 01003*

Synopsis

Tensile stress–strain behavior and dilatation behavior of $CaCO_3$-filled linear polyethylenes with differing molecular weight was found to be dependent upon filler content, polymer filler interface, and polymer molecular weight. Electron microscopy of samples undergoing deformation revealed the presence of craze type deformation.

INTRODUCTION

Particulate inorganic fillers are commonly added to commercial thermoplastic and thermosetting resins to achieve economy as well as favorably modify certain properties such as stiffness, heat distortion, and moldability. However, there is usually a tradeoff involved with certain important properties such as toughness and ultimate elongation, usually deteriorating. The role of polymer molecular weight and crystallinity, filler characteristics (mean particle size and size range), and, most importantly, the effect of the interface on the properties of the composite were studied in this work.

This study investigates the effect of polymer molecular weight, filler volume fraction, and polymer–filler interface on the large strain behavior of $CaCO_3$-filled polyethylene (PE) composites and complements our earlier investigations of the morphology and dynamic mechanical behavior of these composites.[1,2] The changes in stress–strain and dilatation–strain behavior as a function of composite properties and the study of microfailure modes upon deformation by electron microscopy are also discussed.

Another aspect of this study was the investigation of a rather novel composite of ultrahigh molecular weight PE and $CaCO_3$ in powder form available to us from the DuPont Co. The polymer in this composite exhibiting enhanced properties, hereinafter referred as DPCC (DuPont PE/$CaCO_3$ composite), is attached to the filler by means of the polymerization of ethylene monomer on the catalyst coated filler surface.[3,4] This approach to improved polymer–filler interaction may be compared to more conventional techniques wherein the filler surface is coated with "coupling agents" such as silanes and titanates and then compounded with the polymer.

EXPERIMENTAL

Materials. Table I details the origins and relevant properties of the polyethylenes (PE), $CaCO_3$ fillers, and the titanate coupling agent used in this work.

* Present address: Plastics Technical Laboratory, Allied Corporation, Morristown, N. J. 07960.

Journal of Applied Polymer Science, Vol. 28, 2701–2713 (1983)
© 1983 John Wiley & Sons, Inc. CCC 0021-8995/83/092701-13$02.30

TABLE I
Characteristics of Polyethylenes and $CaCO_3$ Used in This Study

A. Polyethylenes	$\bar{M}_w$	$\bar{M}_w/\bar{M}_n$	Crystallinity (%)[a]
LPE Alathon 7050 (E. I. duPont de Nemours and Co.)	57,000	3	83
MPE Marlex 6003 (Phillips Petroleum Co.)	200,000	7–13	75
HPE Hifax 1900[b] (Hercules Powder Co.)	2×10^6	7.6	57
PE portion of DPCC (DuPont PE/$CaCO_3$ composite)[b]	1.5×10^6	3.6	55
B. $CaCO_3$	**$\bar{D}_w$ (μm)**	**$\bar{D}_{max}$ (μm)**	
Atomite (Thompson, Weinman and Co.)	2.5	45	
Atomite Code A (0.5% KRTTS) (Thompson, Weinman and Co.)	2.5	45	
$CaCO_3$ portion of DPCC (DuPont PE/$CaCO_3$ Composite)	2.3	15	
C. Coupling agent			
Isopropyl triisostearyl titanate (KRTTS) (Kenrich Petrochemicals Inc.)			

[a] DSC measurements at 20°C/min scanning rate.
[b] GPC analysis of these samples by Springborn Laboratories, Enfield, Conn.

Sample Preparation. The MPE and LPE composites with $CaCO_3$ were prepared on a two-roll mill at 140–160°C for 5–7 min (depending upon polymer molecular weight). Prior to mixing, the $CaCO_3$ was dried and stored in airtight containers. Compression molding of the milled composites was performed according to ASTM D1928-70 procedure C, using a picture frame mold. Blends of DPCC with MPE and LPE were also prepared using this technique. It must be noted LPE is not suited for such milling operations due to its low molecular weight. HPE is not melt-processible by conventional compounding techniques because of its high melt viscosity. Therefore, mixing of HPE and untreated and treated $CaCO_3$ was carried out by preparing a slurry of the two powders in acetone followed by slowly evaporating the acetone in a Buchi rotary evaporator. Blends of HPE and DPCC were prepared in a similar manner. The high molecular weight PE composites were compression-molded using higher temperatures as recommended by the manufacturer.[5]

ASTM D638 Type C specimens were prepared from 3-mm-thick compression-molded sheets. All specimens were annealed for 1 h at 80°C prior to testing.

Tensile Testing. Stress–strain tests were carried out to the break point using an Instron testing machine at a 5 mm/min stroke rate. Determination of tensile stress at yield (σ_y), tensile stress at break (σ_b), strain at yield (ϵ_y), and strain at break (ϵ_b) was done according to the ASTM D638 procedure.

Dilatation Testing. Stress–strain–dilatation testing was performed using a Farris gas dilatometer.[6] A brief description of its operating principle is given below.

Figure 1 is a schematic of the dilatometer shown in profile. The specimen S

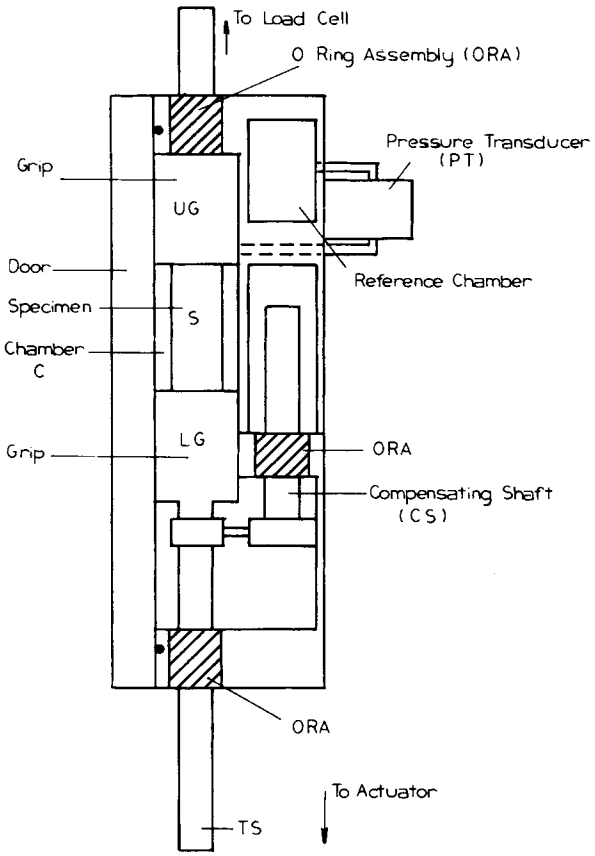

Fig. 1. Schematic of gas dilatometer.

is introduced into a constant volume chamber C and held by the grips UG and LG. The lower grip (LG) is attached to a traveling shaft (TS) which passes through a leak proof O-ring assembly (ORA). To compensate for the volume changes due to TS displacement, an identical shaft (CS) is rigidly attached to the TS. When the sample dilates, the resulting compression of gas in C is measured by a pressure transducer (PT). The transducer was previously calibrated for precise volume changes using a piston micrometer.

The dilatometer as described above was mounted in an Instron servohydraulic testing system (Model 1321). Testing was performed with the tester in stroke control at a stroke rate of 5 mm/min. Sample strain (based on specimen gage length) was limited to 0.50.

Specimens were prepared as follows: previously annealed ASTM D638 C specimens were dipcoated in an ammoniated natural latex for 5 min. They were then dried in air for 30 min, transferred to an air oven maintained at 45°C, and dried overnight. The dried samples were lightly coated with grease prior to testing. The rubber dipcoating prevented diffusion of gas into the specimen while the grease reduced heat transfer between sample and chamber.

Deformation Microscopy. Small dogbone-shaped specimens (0.75 mm × 1 mm × 0.1 mm) were mounted on specially prepared copper deformation grids, coated with gold, and stretched in an electron microscope (JEOL 100 CX Tem-

scan) using a deformation grid holder. The specimens were observed in the secondary electron imaging mode.

RESULTS AND ANALYSIS

Tensile Testing

The results of tensile tests are shown in Table II.

Unfilled Polyethylenes. The polyethylenes studied were chosen to represent a wide range of molecular weight so as to determine the role of matrix molecular weight on the ultimate properties of the filled polymer.

LPE, once annealed under the conditions described above, was found to exhibit negligible extension after yield. MPE specimens exhibited a necking, and the samples extended to 530% by drawing. Necking and consequent drawing of HPE specimens was not observed. Instead, after yielding, the slope of the stress–strain curve remained positive, and the samples were found to extend by uniform reduction of cross-sectional area. It may be expected that such differences in mechanical behavior are a result of morphological differences in the sample resulting from the variation of molecular weight. Unfilled LPE samples exhibited visually flat fracture surfaces while MPE fractured creating uneven fibrillated surfaces. HPE fracture surfaces were also quite flat. However, there was distinctive recoil of the two halves of the HPE sample upon breaking, indicating a distinct entropic character in the deformation of the high molecular weight polyethylene.

DPCC. DPCC exhibits a sharp yield at a relatively low strain of 4%. Beyond this strain value, it extended with no necking until break (410%). The similarity of the stress–strain curve to that of an impact-modified, glassy thermoplastic is noteworthy.

Filled LPE. Since the unfilled low molecular weight LPE is itself not ductile, it is not surprising that the filled specimens exhibited similar behavior. Treatment of the $CaCO_3$ surface with KRTTS improved elongation at break, as did blending of LPE with DPCC composite.

Filled MPE. In general both yield stress (σ_y) and elongation at break (ϵ_b) decreased with increasing amount of filler. The treatment of $CaCO_3$ with KRTTS (treated $CaCO_3$) had a significant effect on both σ_y and ϵ_b. The yield stress of treated $CaCO_3$ filled PE's is less than that of the untreated at the same filler loading. Also, the elongation at break improves greatly when the $CaCO_3$ is treated at all filler loadings investigated. Filled MPE specimens also exhibited necking, though it becomes less pronounced with increasing filler content. The yield stress and elongation at break of DPCC composite blends do not indicate a trend, although elongations at break are lower than treated $CaCO_3$-filled specimens. This is believed to be due to imperfect mixing of DPCC with MPE due to the high melt viscosity of DPCC.

Filled HPE. Blends of HPE with DPHC display good mechanical properties with high elongations at break. However, blends of HPE with treated and untreated $CaCO_3$ exhibited properties that rapidly deteriorated with increased filler loading. There is little doubt that this deterioration is due to filler agglomeration caused by limited mobility of HPE resulting in a poor dispersion.

TABLE II
Tensile Properties of Filled Polyethylenes[a]

	σ_y (MN/m^2)			ϵ_y %			σ_D (MN/m^2)			ϵ_b (%)		
	U	T	B	U	T	B	U	T	B	U	T	B
LPE	19.1			6			13.3			9		
+2% $CaCO_3$		23.5					22.6	23.5	21.4	9	23	8
+4% $CaCO_3$						13	22.0	22.2	24.6	7	15	16
+8% $CaCO_3$						10	14.7	19.8	22.5	4	15	12
+19% $CaCO_3$							12.68			3	3	
MPE	24.6			22			12.9			530		
+2% $CaCO_3$	25.6	24.6	23.9	20	20	20	8.6	12.3	14.7	140	290	410
+4% $CaCO_3$	23.4	21.4	22.4	25	18	18	7.5	16.8	17.9	92	394	120
+8% $CaCO_3$	22.2	20.4	28.3	14	15	20	7.0	13.3	18.5	100	300	106
+19% $CaCO_3$	17.9	14.9		6.4	14		18.2	13.0			42	
HPE	21.5			28			28.1			820		
+2% $CaCO_3$	17.0		16.4	20		13	21.2		22.7	595		344
+19% $CaCO_3$	13.5	11.6	14.7	12	12	10	13.7	12.1	20.0	20	20	614
DuPont PE/$CaCO_3$ composite (38% $CaCO_3$)	12.4			4			12.6			410		

[a] U = untreated $CaCO_3$; T = $CaCO_3$ + 0.5% KRTTS; B = blend of PE and DuPont composite.

Dilatation Measurement

Figures 2, 3, 4, and 5 present dilatation behavior of the filled polyethylenes tested. LPE and its composites gave negligible dilatation before break. Figure 2 compares the stress–strain and dilatation–strain behavior of $CaCO_3$-filled MPE at 0%, 2%, 4%, 8% and 19% by volume of filler. Dilatation commences at about the yield point of the specimen and increases with filler content. The dilatation curves change slope at strains between 0.3 and 0.4. Similar results are seen for KRTTS-treated $CaCO_3$, for $CaCO_3$-filled HPE, and for blends of HPE and DPHC.

DISCUSSION

Tensile Testing

Nicolais and Narkis[7] proposed a model for filler well dispersed in glassy matrices based on dewetting reducing effective cross-sectional area:

$$\sigma_{yf} = \sigma_{yp}(1 - 1.21\phi^{2/3}) \tag{1}$$

where σ_{yf} and σ_{yp} are the yield stress of filled and unfilled polymer, respectively, and ϕ is the volume fraction of filler.

Figure 6 is the plot of σ_{yc}/σ_{yp} against ϕ for filled MPE. Good agreement with eq. (1) was exhibited by MPE filled with treated $CaCO_3$ and may be the result of better dispersion of the treated $CaCO_3$ in the matrix. The better dispersion achieved with treated $CaCO_3$ leads to a greater reduction of load bearing area

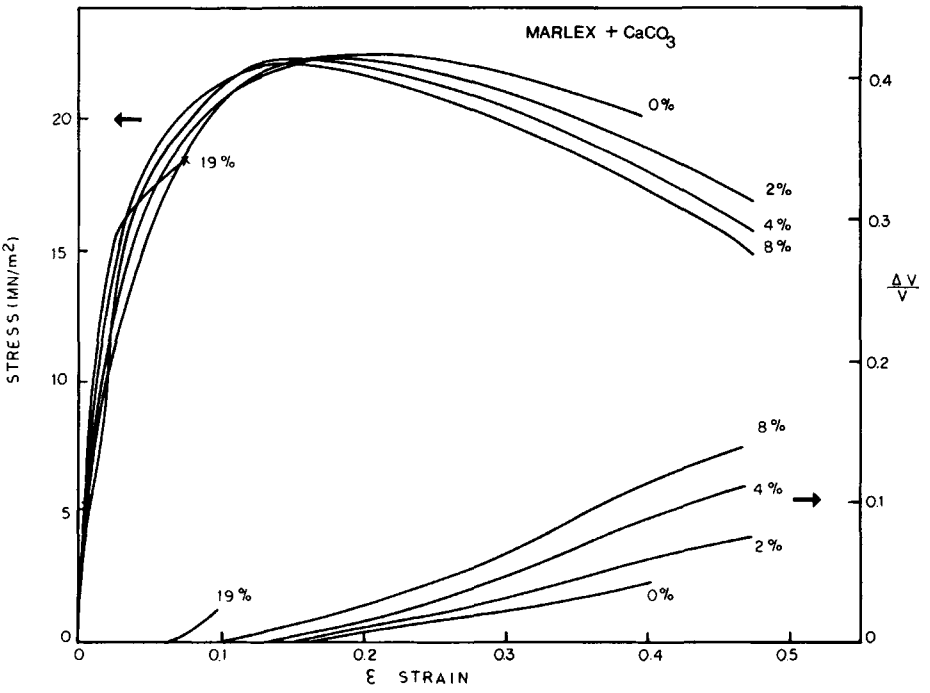

Fig. 2. Stress–strain–dilation curves for MPE filled with 0, 2, 4, 8, and 19 vol % $CaCO_3$.

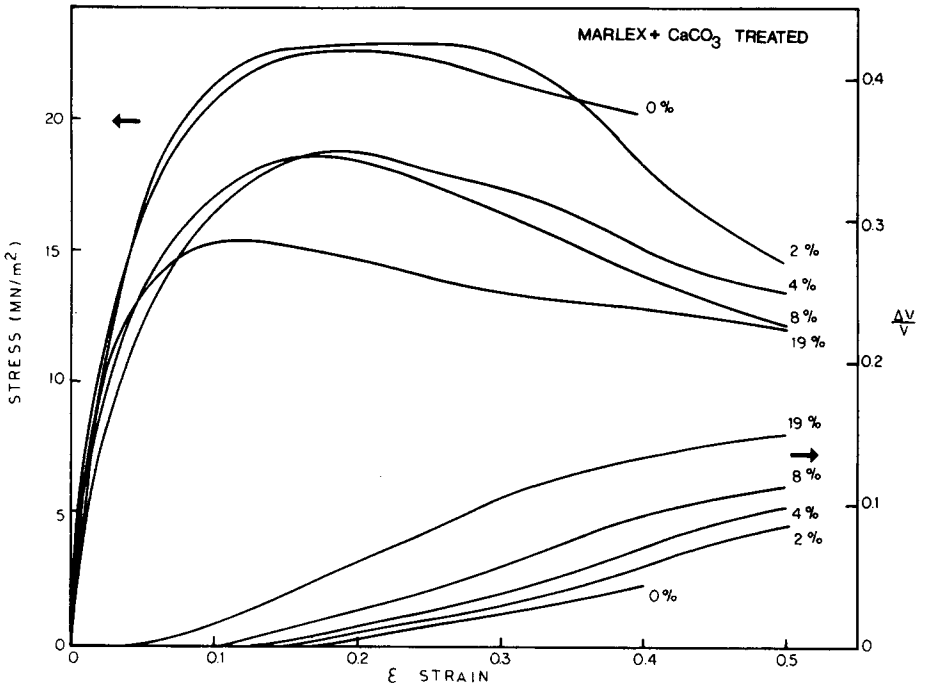

Fig. 3. Stress–strain–dilation curves for MPE filled with 0, 2, 4, 8, and 19 vol % treated $CaCO_3$.

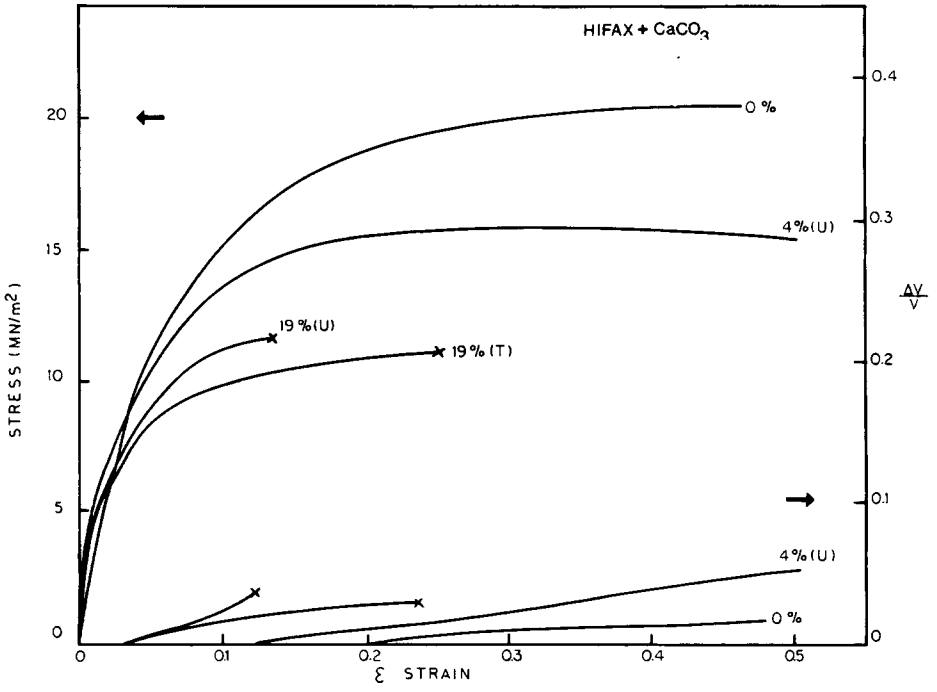

Fig. 4. Stress–strain–dilation curves for HPE filled with 0.4 and 19 vol % $CaCO_3$ (U) and 19 vol % treated $CaCO_3$ (T).

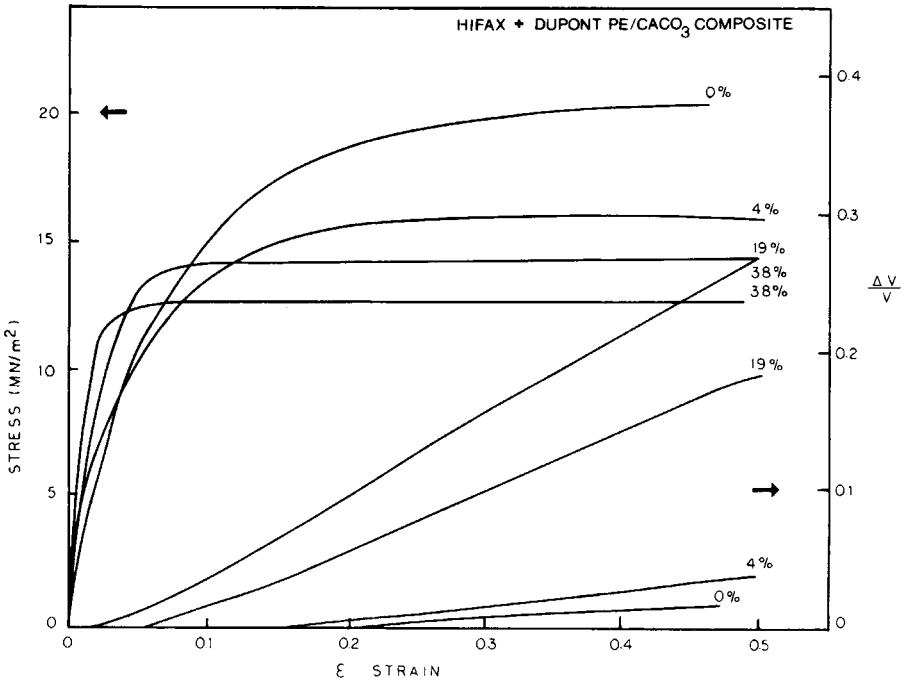

Fig. 5. Stress–strain–dilation curves for HPE blended with DPCC. The blends contain 0.4 and 19 vol % $CaCO_3$. Also shown is DPCC (38 vol % $CaCO_3$).

upon dewetting as compared to the poorly dispersed untreated $CaCO_3$ case. The reduction of yield stress upon treatment of filler surface has been observed in other studies of $CaCO_3$-filled polyethylene and polypropylene.[8,9]

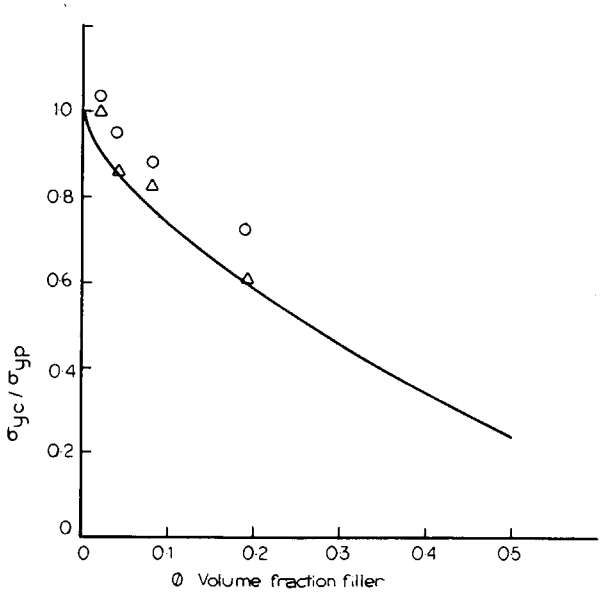

Fig. 6. Comparison of experimental data with Nicolais–Narkis expression for yield point determination: (○) Marlex + 19 vol % $CaCO_3$; (△) Marlex + 19 vol % treated $CaCO_3$; $\sigma_{yc}/\sigma_{yp} = (1 - 1.21\ \phi^{2/3})$.

Dilatation

Figure 7 illustrates the effect of $CaCO_3$ surface treatment with KRTTS and shows the stress–strain–dilatation curves of MPE filled with 4% and 8% $CaCO_3$ both untreated and treated. The dilatation curves coincide at low strains; however, at higher strains the specimens filled with untreated $CaCO_3$ exhibit higher dilatation.

Volume creating microfailure modes are observed at large strains in polymer blends and composites where phase boundaries exist. Vacuoles and crazes are two types of volume creating microfailure modes considered here. Farris[10] proposed a stochastic model to account for dilatation in filled elastomers based on the fact that ellipsoid shaped vacuole formation was observed around spherical filler particles. It is shown that the maximum slope of the dilatation–strain curve is proportional to volume fraction of filler around which vacuoles exist (the modeling of vacuoles assume there are no load bearing polymer fibrils, a point of difference from crazes):

$$\frac{1}{v_0}\left(\frac{d(\Delta v)}{d\epsilon}\right) = Cv_f \tag{2}$$

where v_0 is the volume of sample undergoing dilatation, ϵ the longitudinal strain, and v_f the volume fraction of filler present. At steady state the constant C was experimentally found to be 1 in filled elastomers.

Bucknall has measured dilatation in rubber modified thermoplastics utilizing the Darlington and Saunder extensometer arrangement.[11] Bucknall made the assumption that crazing and shear yielding are the only mechanisms responsible for deformation beyond the elastic region and, upon considering shear yielding

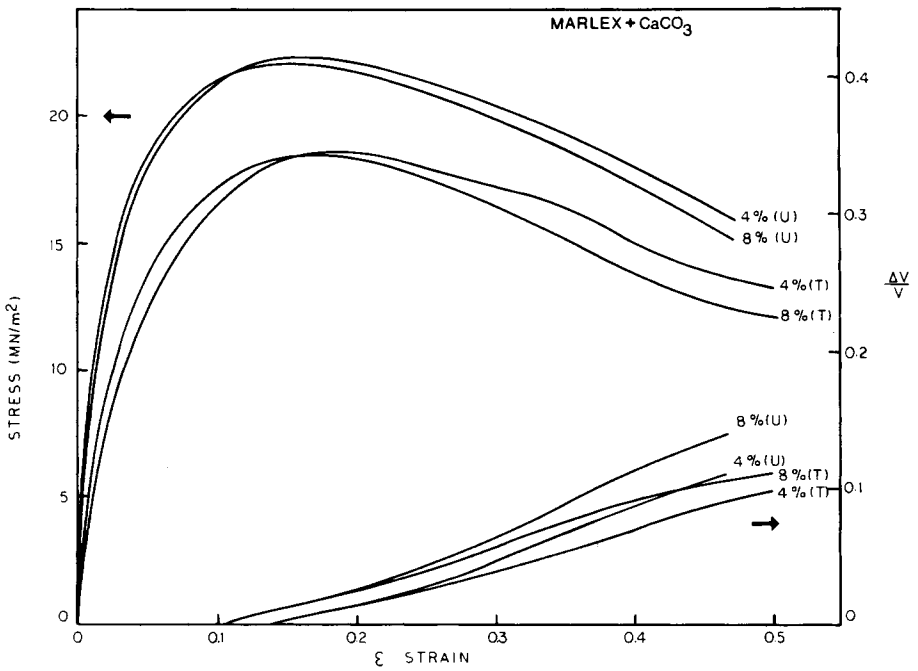

Fig. 7. Effect of filler treatment on stress–strain–dilation curves. Shown are MPE filled with 4 and 8 vol % $CaCO_3$ untreated (U) and treated (T).

TABLE III
Slopes of Dilatation–Strain Curves for Filled MPE Specimens

Sample	Maximum slope	
	Untreated $CaCO_3$	Treated $CaCO_3$
MPE	0.17	
+2%	0.20	0.20
+4%	0.30	0.25
+8%	0.35	0.30
+19%	0.60	0.50

to be essentially a volume conserving mode of deformation, showed that the slope of the dilatation–strain curve is related to the extent of crazing:

$$\frac{1}{v_0}\left(\frac{d\Delta v}{d\epsilon}\right) = 1 + 2\frac{\partial \epsilon_2}{\partial \epsilon_1} \tag{3}$$

where ϵ_2 is lateral strain and the other symbols have their usual meaning. Hence, if there is no shear yielding, the slope of the curve would be 1, and, if shear

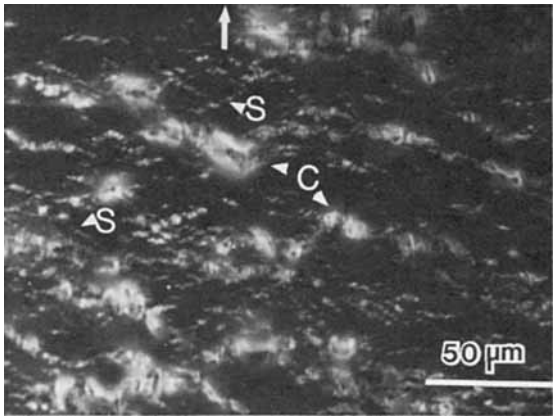

(a)

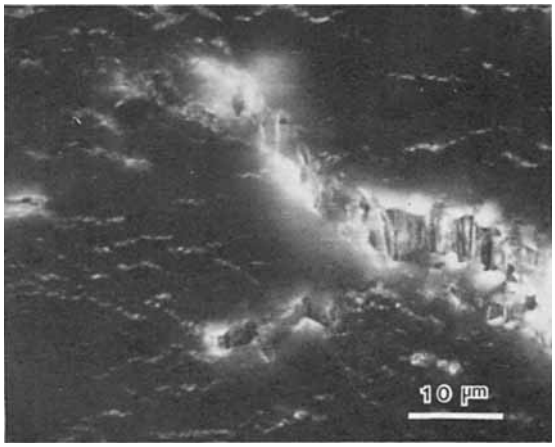

(b)

Fig. 8. (a) Scanning electron micrograph of $CaCO_3$-filled MPE showing two modes of failure: crazes (C) and shear zones (S). (b) Higher magnification view of the neighborhood of a craze.

yielding totally dominated deformation, the slope would equal zero. While no assumption is made regarding the geometry of the craze in this equation, morphological investigations reveal crazes in impact-modified thermoplastics to develop and grow normal to the stress direction.

In Table III are given values for the slopes of the dilatation–strain curves of MPE filled with $CaCO_3$. It is noticed that the slopes of the curves indicates increasing amounts of dilatational microfailure in the steady state regions (the slope of the curve is independent of the sample gage length). A maximum value of 45% dilatational failure is observed at 19 vol % filler loading. Hence dilatational failure greatly exceeds that predicted by eq. (2).

In order to investigate the type of dilatational failure mode present in rigid particle-filled semicrystalline polymer the deformation morphology of filled and unfilled polyethylenes was investigated. While the conclusions of the entire study will be published separately a few pertinent results are indicated here. In Figure 8 are two scanning electron micrographs–secondary electron images (SEM–SEI's) of MPE filled with $CaCO_3$. In Figure 8(a) the lower magnification micrograph of two distinct forms of microfailure are seen and are denoted as C (crazes) and S (shear zones). The crazes (c) are characterized by a void–fibril structure with dominant dimension normal to the direction of applied tensile stress. Associated with the crazes are seen large dewetted $CaCO_3$ particles. Shear

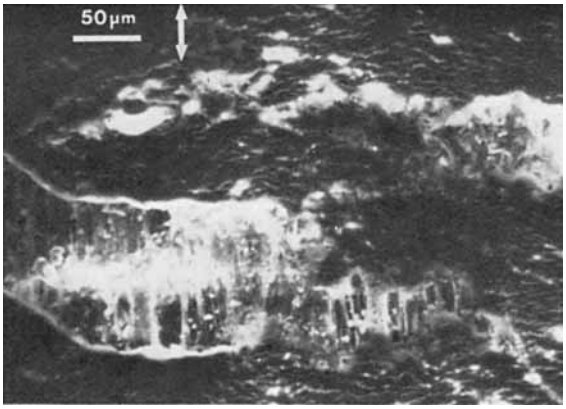

(a)

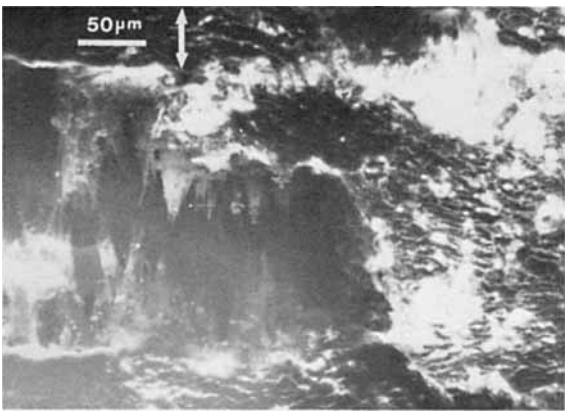

(b)

Fig. 9. (a) Critical craze in $CaCO_3$-filler MPE; (b) same region after failure.

zones are smaller in size, more profuse, and even at high magnification do not appear to possess marked fibrillar character.

The two deformation modes are seen more clearly in Figure 8(b), which is a higher magnification image of a region of Figure 8(a). Here the fibrillated nature of the crazes is more distinctly revealed. Figures 9(a) and (b) show the critical craze in a MPE/$CaCO_3$ sample. Fully dewetted particles are evident in the midsection of the craze. It is also noticed that shear yielding has occurred in region S. The angle the shear bands make is in the range 20–45° to the loading direction.

It is easier to visualize dewetting (vacuole formation) when the inclusions in a composite are rigid relative to the matrix since the stress concentrations occur at the poles and, subsequently, the matrix separates from the filler in that region. For crazes to occur, however, the stress concentration must occur in the equatorial regions, and this is possible when the modulus of the inclusion is less than that of the matrix as in impact-modified thermoplastics.

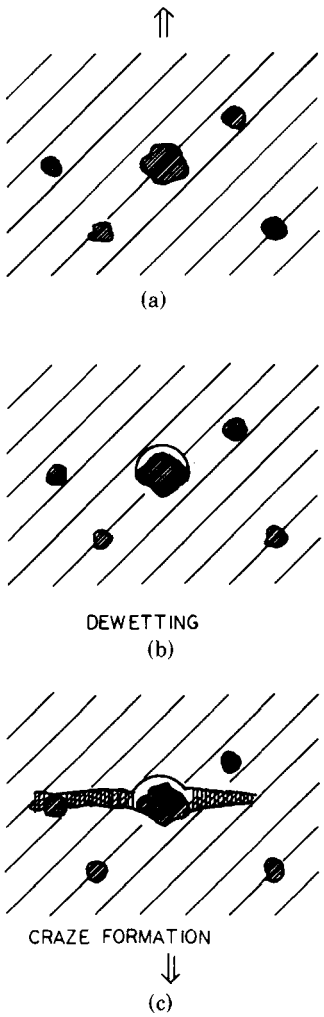

Fig. 10. Schematic for proposed craze formation process in filled PE: (a) initial configuration; (b) dewetted particle; (c) craze formation normal to the stress direction.

A possible explanation for crazing in filled semicrystalline thermoplastics could indeed visualize both mechanisms operating and this is shown in Figures 10(a), (b), and (c). Initially particles could dewet [Fig. 10(b)]. Subsequently, the stress concentrations would shift to the equatorial region since the void is nonreinforcing. Given the irregular shape of the particles, a profile of the void in the equatorial region would accelerate the formation of a craze [Fig. 10(c)]. After the crazes attain certain dimensions, their growth would dominate the dewetting process in the dilatational response of the specimen.

It is expected that improved dispersion would lead to a greater number of localized crazes. However, their dimensions would be smaller than crazes initiated by regions of agglomerated particles, and their dilatation would also be less. This has been noted by Farris earlier.[10] This would explain the differences in dilatational behavior of untreated and treated $CaCO_3$-filled polyethylene at large strains.

CONCLUSIONS

The mechanical properties of three polyethylenes filled with $CaCO_3$ were found to be dependent upon filler content, polymer–filler interface, and polymer molecular weight. Increase in filler content reduced both yield stress as well as elongation at break. Treatment of $CaCO_3$ with a titanate coupling agent improved elongation at break but decreased yield stress, both effects attributable to improved dispersion. Increase in polymer molecular weight resulted in increase in elongation at break accompanied by a transformation of the large strain deformation from a ductile mode to a rubbery one.

Dilatation of specimens increased with $CaCO_3$ content. Dilatation at high strains was suppressed when the $CaCO_3$ was treated with the titanate. An electron microscopy observation of the deformation of unfilled and filled specimens revealed that crazes (void–fibril structures) are present in deformed filled polyethylene.

The authors are grateful to E. G. Howard of the E. I. DuPont Co. for making available experimental quantities of the novel composite discussed in the text. This work was supported by AFOSR 81-0101 and the Materials Research Laboratory.

References

1. V. P. Chacko, F. E. Karasz, R. J. Farris, and E. L. Thomas, *J. Polym. Sci., Polym. Phys. Ed.*, **20,** 2177 (1982).
2. V. P. Chacko, F. E. Karasz, and R. J. Farris, *Polym. Eng. Sci.*, **22,** 968 (1982).
3. U. S. Pat. 3,950,303 (1977) issued to R. D. Lipscomb of E. I. DuPont de Nemours and Co.
4. E. G. Howard, B. L. Glazar, and J. W. Collette, *Ind. Eng. Chem., Prod. Res. Dev.*, **20,** 421 (1981).
5. Hercules Powder Co., Hifax 1900 product literature.
6. R. J. Farris, *J. Appl. Polym. Sci.*, **8,** 25 (1964).
7. L. Nicolais and M. Narkis, *Polym. Eng. Sci.*, 11(3), 194 (1971).
8. S. J. Monte and G. Sugerman, Kenrich Petrochemicals Bulletin KR-1079-9, 1979.
9. Thompson, Weinman and Co., Technical Bulletin T-5-6,8, 1981.
10. R. J. Farris, Trans. Soc. Rheol., **12**(2), 315 (1968).
11. C. B. Bucknall, *Toughened Plastics*, Applied Science, London, 1977.

Received May 20, 1982
Accepted April 27, 1983